CENTER FOR COMPUTATIONAL RELATIVITY AND GRAVITATION

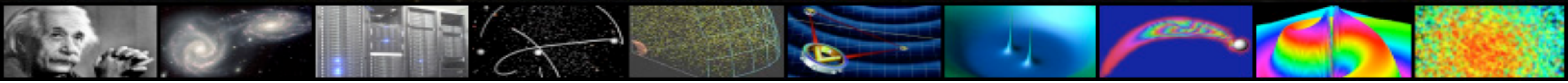

Spin-flips in Black Hole Binaries

Carlos Lousto
and James Healy, Hiroyuki Nakano
Rochester Institute of Technology

Oxford, MS February 28th 2017

10+ years of Numerical Relativity Breakthrough

What have we learn about the dynamics of orbiting spinning binary black holes?

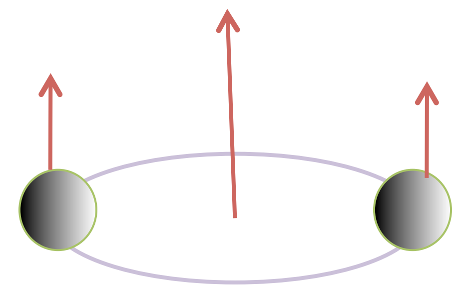

- The spin *hang-up* effect (delaying) the merger of two black holes prevents the formation of naked singularities (Cosmic Censorship).

- The final larger black hole may acquire speeds up to 5000 km/s due to radiation of gravitational waves. This is the *hung-up recoil* effect .

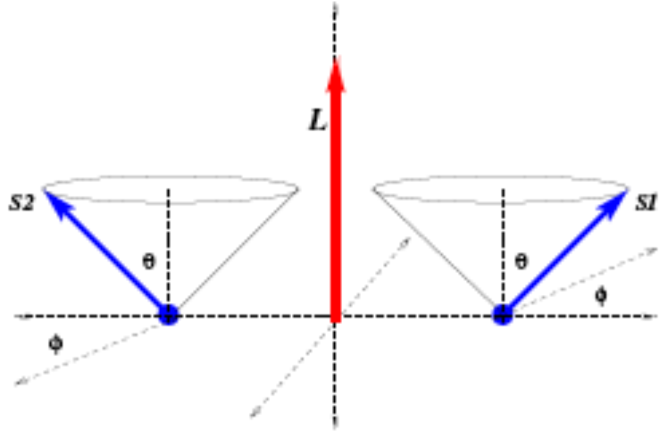

Numerical simulation

Motivation: To further understand the dynamics of spinning (precessing) binary black holes

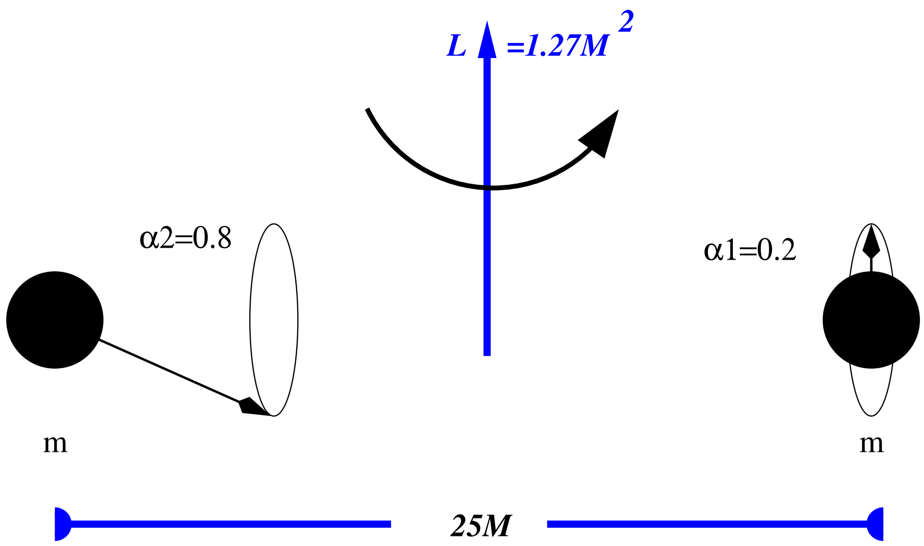

Equal mass binary with initial proper separation d=25M.
Unequal spins α_1=0.2 aligned with **L**
α_2=0.8 slightly misaligned with L such that **S**.**L**=0.

Run lasts for t=20,000M and makes 48.5 orbits before merger, 3 cycles of precession and one half of spin-flip.

After merger the final black hole acquires a recoil velocity of 1500 km/s.

Based on: C.O.Lousto & J.Healy, Physical Review Letters, **114**, 141101 (2015)

Orbital Precession

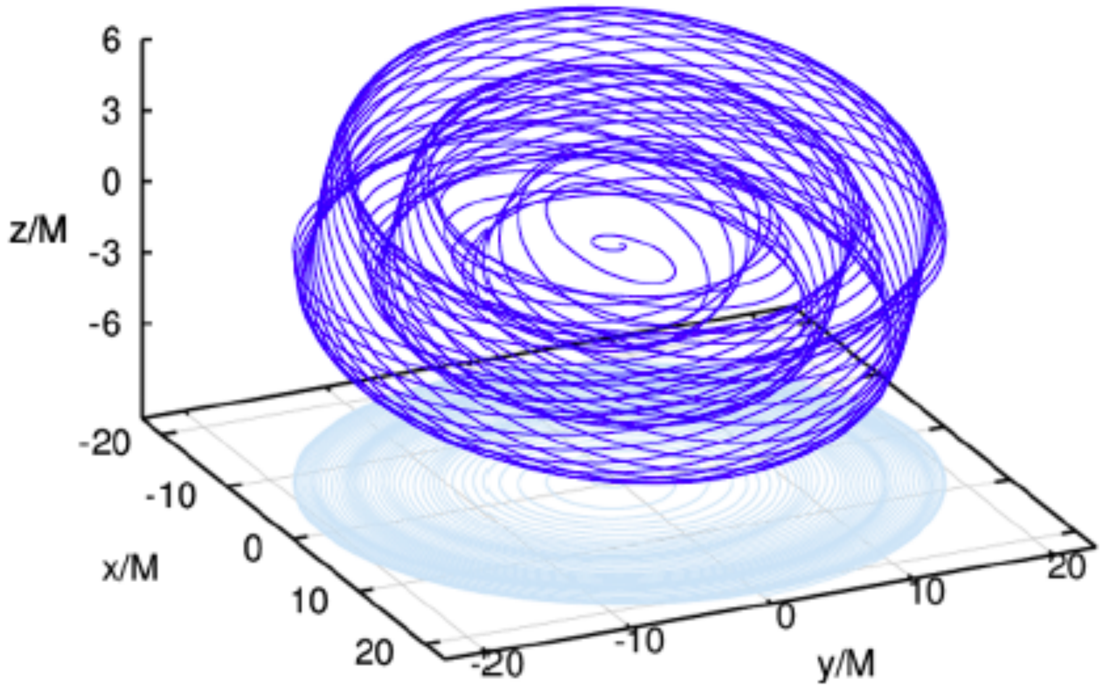

FIG. 2. Precession of the orbital plane as displayed by the distance vector $\vec{d} = \vec{x}_1(t) - \vec{x}_2(t)$.

Eccentricity radiation

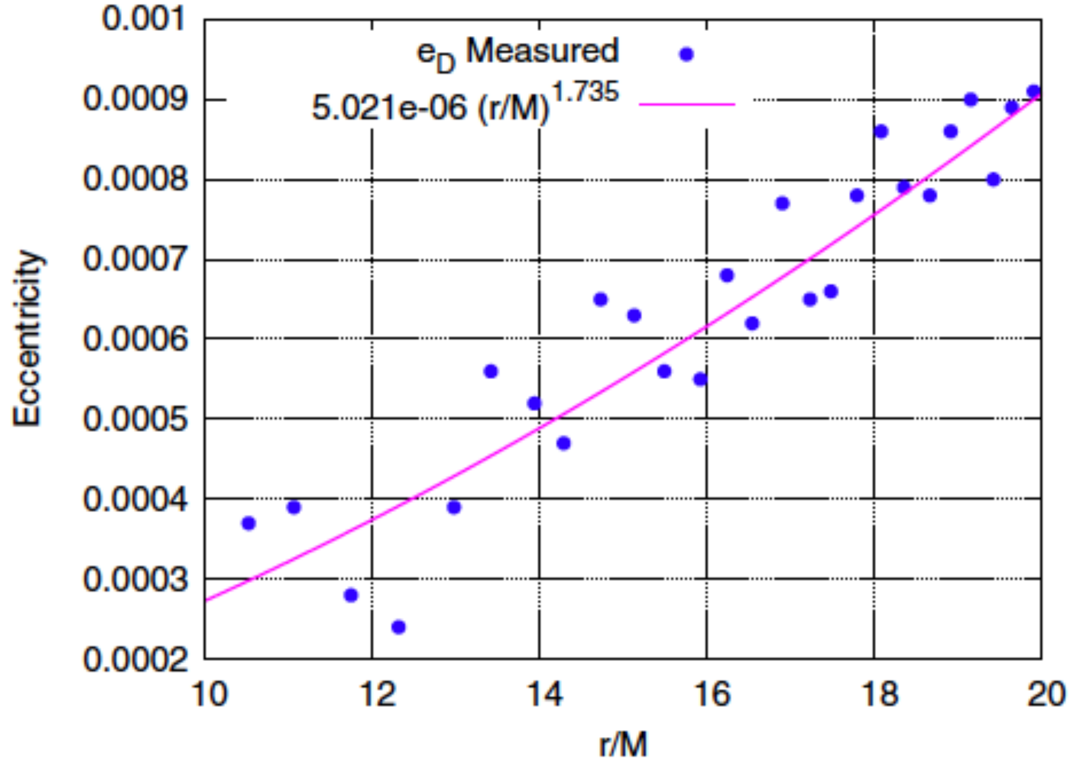

FIG. 9. Evolution of the eccentricity versus coordinate separation of the BHB. Dots represent measurements of the eccentricity, e_D, and the continuous curve a fit to its decay with $e \sim r^{1.73486 \pm 0.1495}$. In comparison, the theoretical prediction is $e \sim r^{1.5833}$.

Spin Evolution

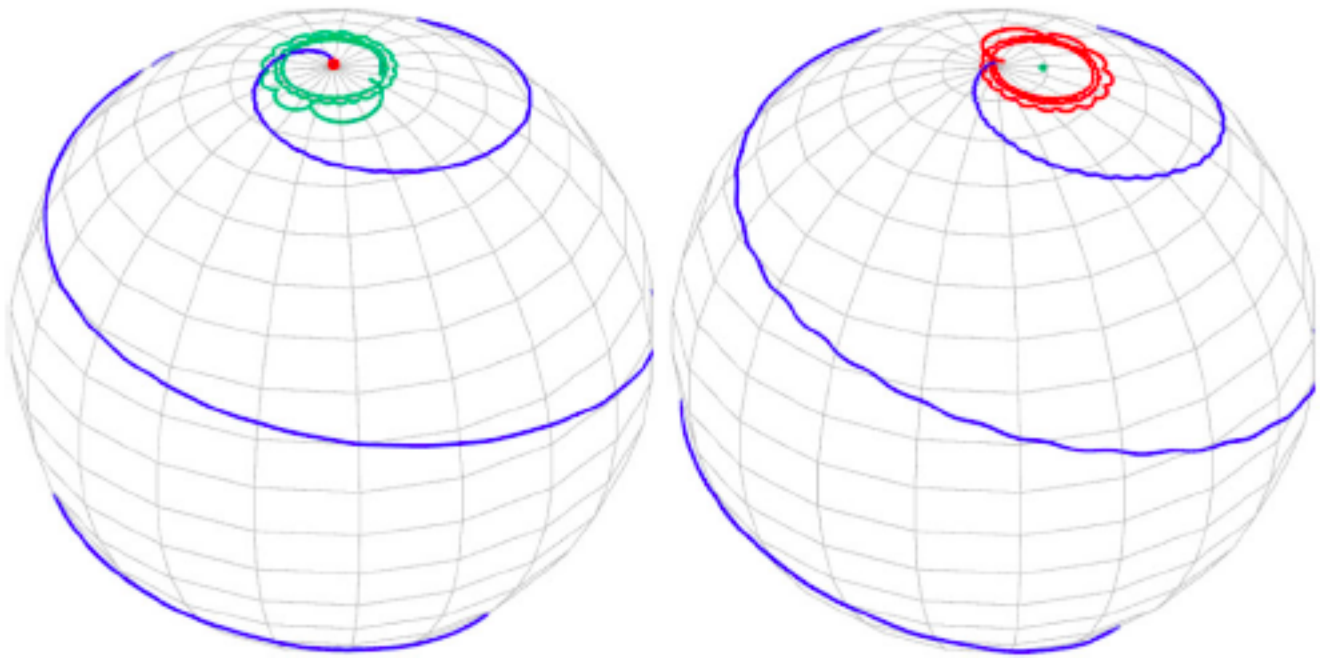

FIG. 5. Change in the spin direction (in blue) of the BH1 (with the smaller spin magnitude) in the orbital frame, $\hat{L}$ (left), and the coordinate frame $\hat{z}$ (right). Plotted also the directions of $\vec{L}$ in red and $\vec{J}$ in green.

Waveforms

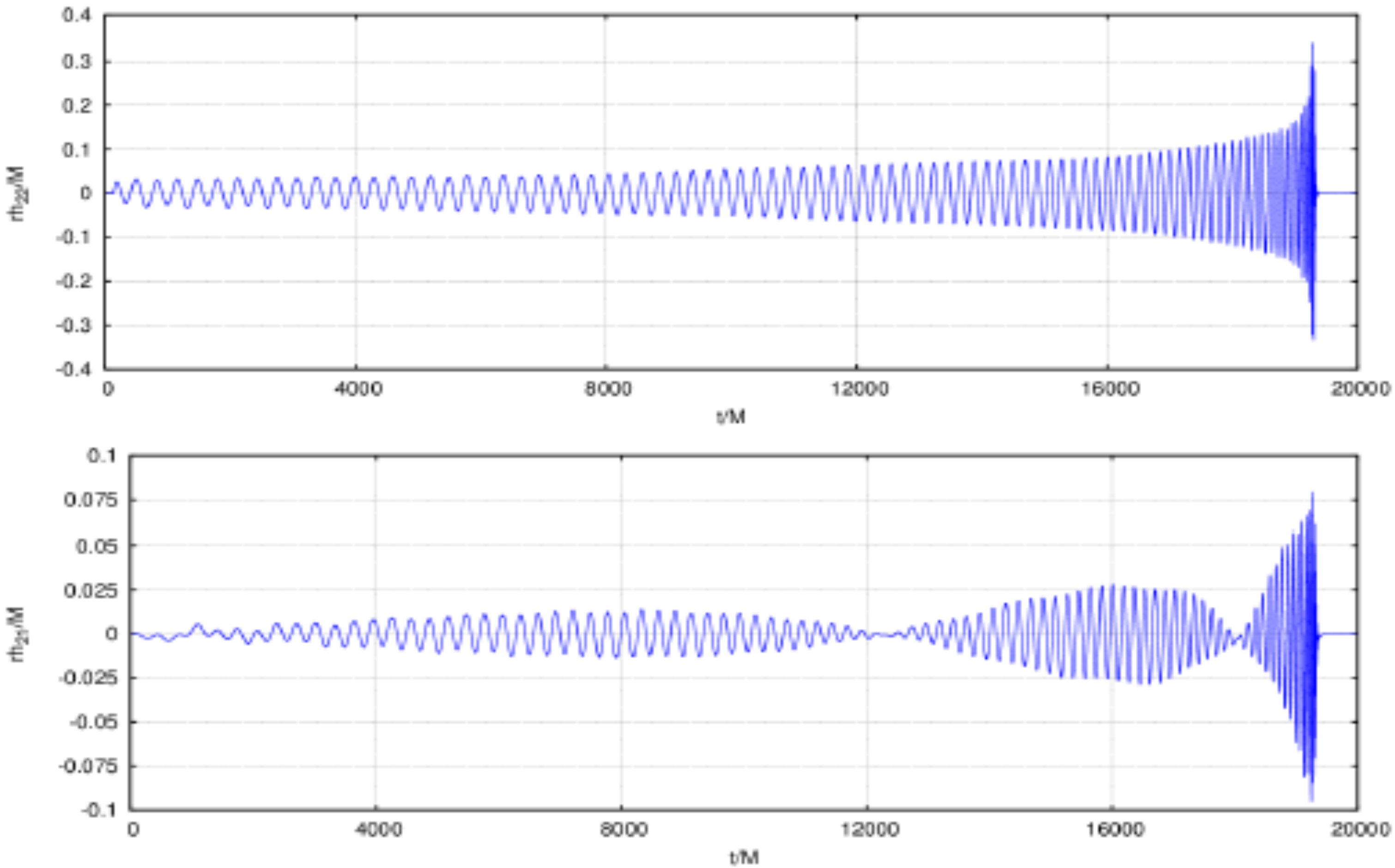

FIG. 3. The real part of the waveform strain for the modes $(\ell, m) = (2,2)$ and $(\ell, m) = (2,1)$. While the former (top) gives the leading chirping amplitude, the latter (bottom) clearly displays the precession effect, completing nearly three cycles during the $t = 20000M$ of the simulation.

2PN Spin dynamics

From $$\frac{d\vec{S}_1}{dt} = \frac{1}{r^3}\left[\left(2+\frac{3}{2q}\right)\vec{L} - \vec{S}_2 + \frac{3(\vec{S}_0\cdot\hat{n})}{1+q}\hat{n}\right]\times\vec{S}_1,$$

$$\frac{d\vec{S}_2}{dt} = \frac{1}{r^3}\left[\left(2+\frac{3q}{2}\right)\vec{L} - \vec{S}_1 + \frac{3q(\vec{S}_0\cdot\hat{n})}{1+q}\hat{n}\right]\times\vec{S}_2,$$

where $\vec{n} = \vec{r}_1 - \vec{r}_2$ and

$$\vec{S}_0 = \left(1+\frac{1}{q}\right)\vec{S}_1 + (1+q)\vec{S}_2.$$

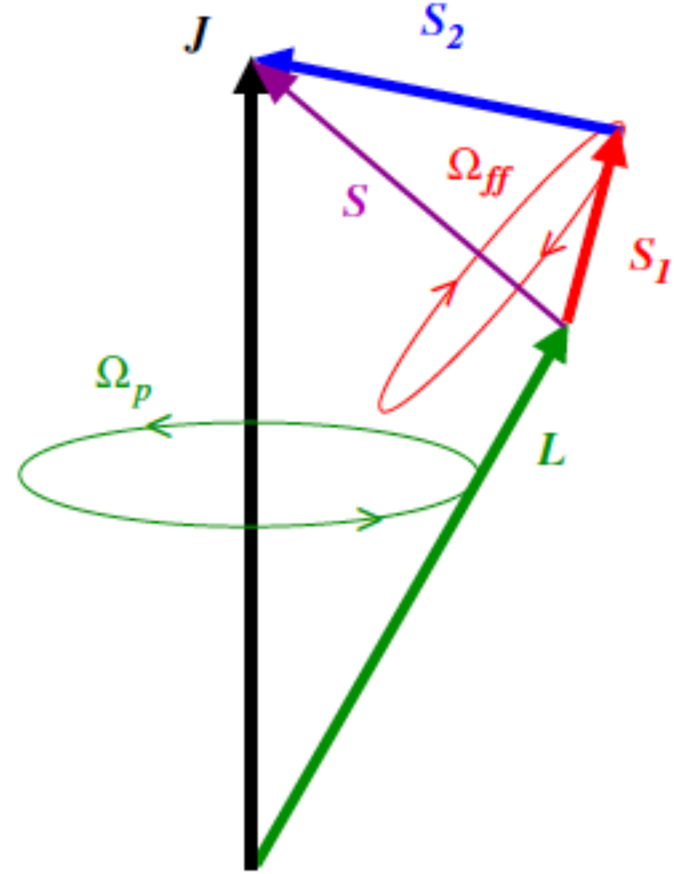

We obtain the polar and azimuthal frequencies with respect to

$$\Omega_{ff} = 3\frac{S}{r^3}\left[1 - \frac{2\vec{S}\cdot\hat{L}}{M^{3/2}r^{1/2}}\right],$$

$$\Omega_p = \frac{7L}{2r^3} + \frac{2}{r^3}(\vec{S}\cdot\hat{L}),$$

The flip-flop happens when both spins are non-vanishing.

Unequal mass spinning binaries: 2PN analysis

The flip-flopping frequency leading terms are now,

$$M\Omega_{1,2}^{ff} \approx \frac{3}{2}\frac{|1-q|}{(1+q)}\left(\frac{M}{r}\right)^{5/2} + 3\frac{S_1^L - S_2^L}{M^2}\left(\frac{M}{r}\right)^3 sign(1-q)$$

The origin of the additional term for unequal masses scaling with $\sim r^{-5/2}$ is due to the non-conservation of the angle β between the two spins (as opposed to its conservation in the $q=1$ case). These oscillations in β are due to the differential precessional angular velocity of $\vec{S}_1$ and $\vec{S}_2$ for $q \neq 1$ and hence provides the (precessional) scaling $r^{-5/2}$.

The maximum flip-flop angle is now,

$$1 - \cos(\Delta\theta_{1L}^{ff}) \approx \frac{2\alpha_2^2}{(1-q)^2}\left(\frac{M}{r}\right) + \frac{4\alpha_1\alpha_2^2 q}{(1-q)^3}\left(\frac{M}{r}\right)^{3/2}$$

Unequal mass spinning binaries: 3.5PN Evolution Probabilities

below. These results are for initial random spin distributions evolved with 3.5PN form $100M$ of initial separation down to $5M$ (approximating the merger).

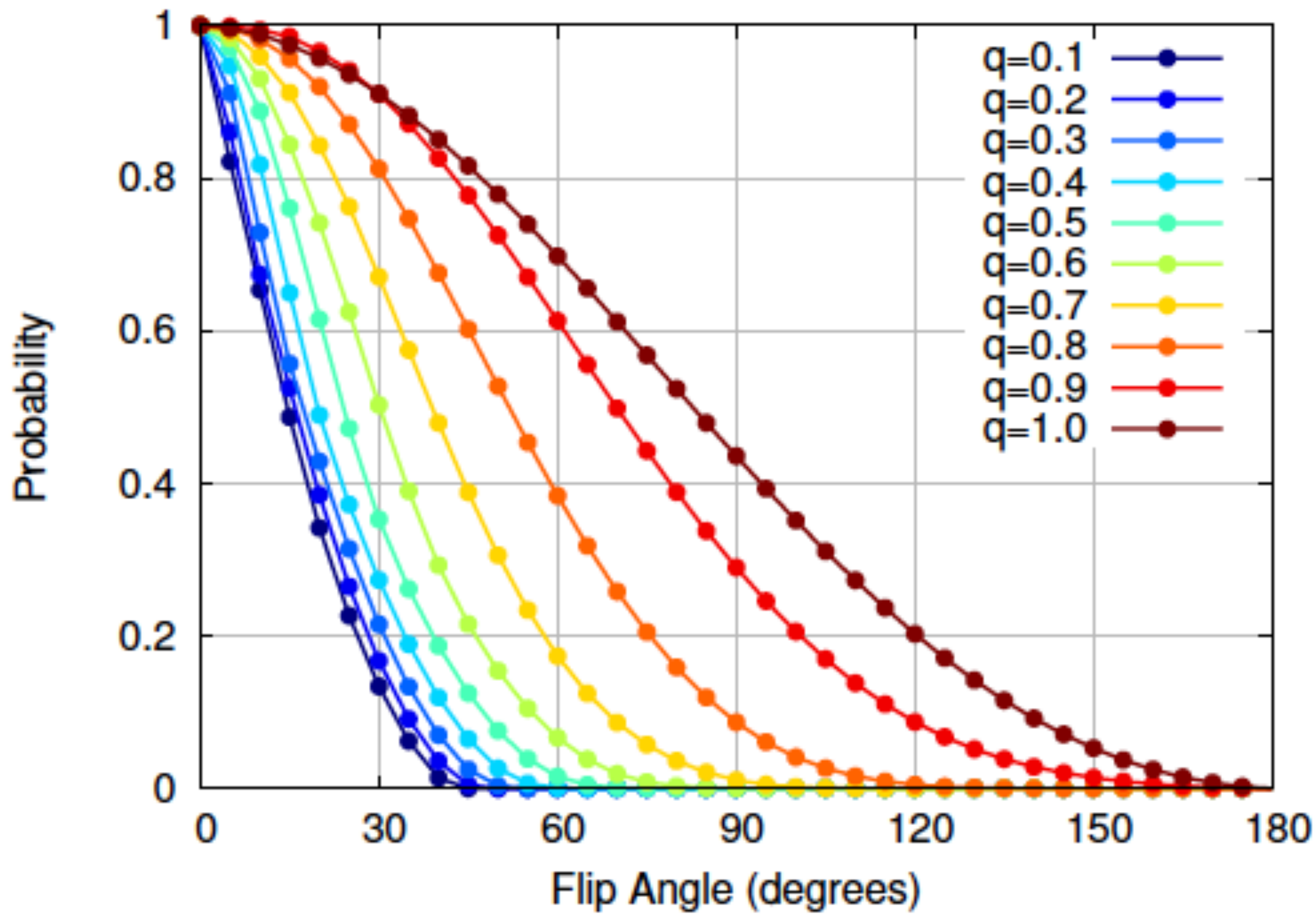

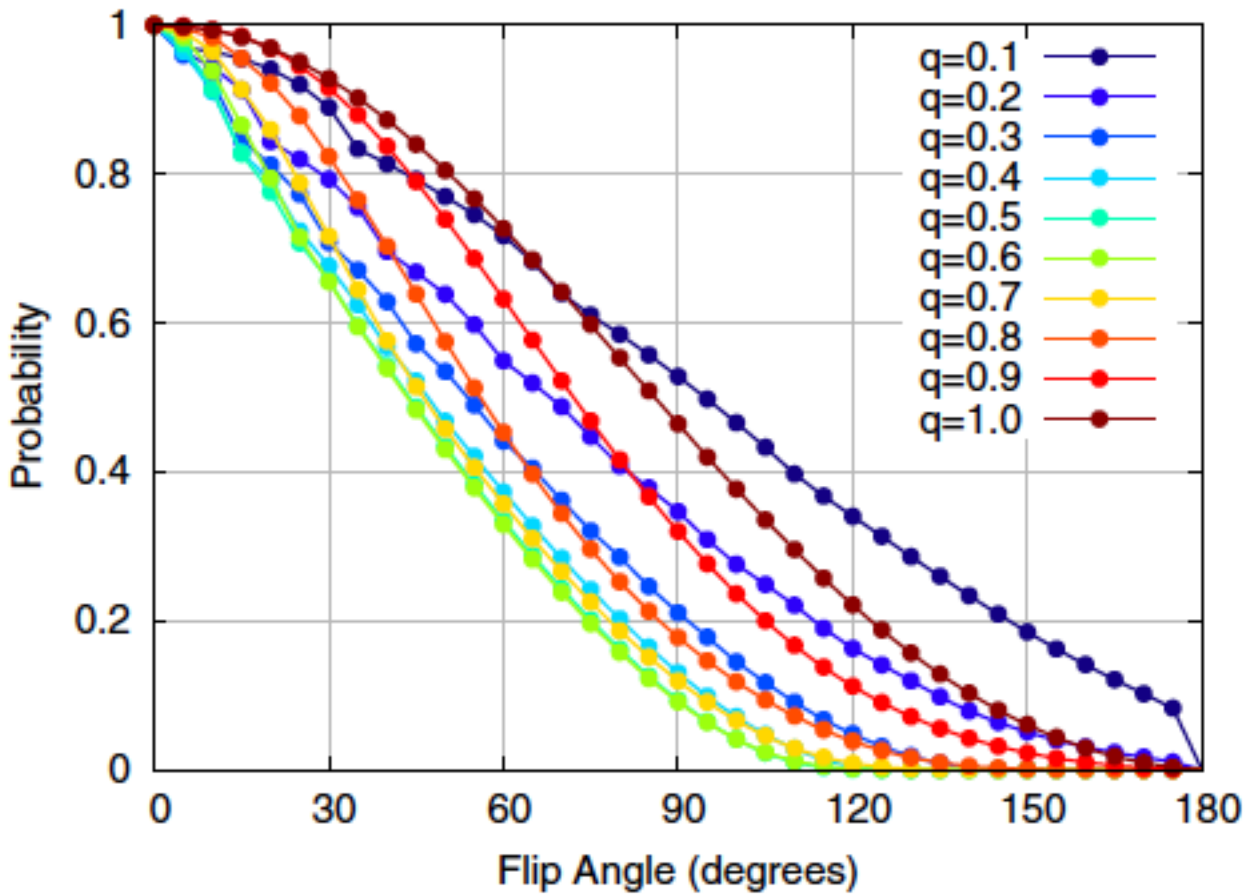

In Fig. 22 we display the differences for a few selected mass ratios. We observe in general that larger angles are seen in the J-frame. Particularly for $q = 0.1$, due to the effects of transitional precession [63], that may reverse the orientation of $\vec{J}$. But we also observe larger angles for $q > 1/4$,

Discussion: Observational effects

The leading flip-flop period is now given by

$$T_{ff} \approx 2,000\, yr \, \frac{(1+q)}{(1-q)} \left(\frac{r}{1000M}\right)^{5/2} \left(\frac{M}{10^8 M_\odot}\right).$$

which is much shorter than the gravitational radiation

$$T_{GW} \approx 1.22\, 10^6\, yr \left(\frac{r}{1000M}\right)^4 \left(\frac{M}{10^8 M_\odot}\right),$$

alignment processes can be less effective than expected when the flip-flop of spins is taken into account.

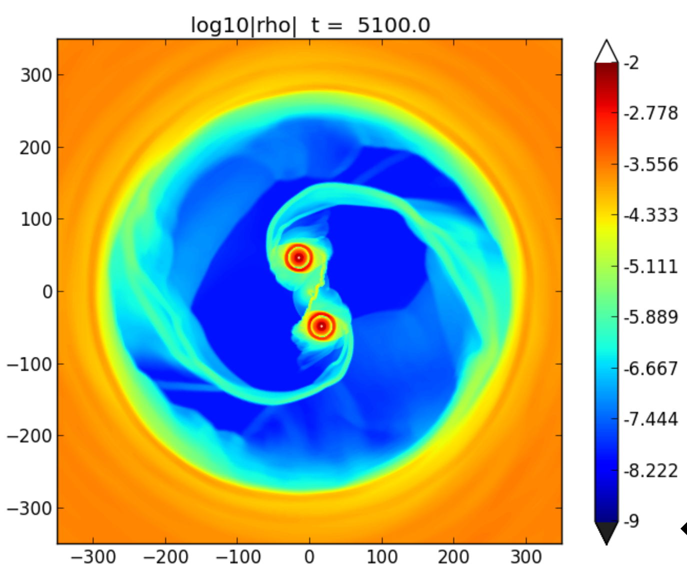

← Simulation by RIT group

Accretion disk internal rim will change location with spin orientation. This changes

- Efficiency of the EM radiation
- Spectrum of EM radiation (hard part)
- Cutting frequency of oscillations

Proper modeling using GRMHD simulations

X-shaped galaxies should show 'orange peeling' jets when they were about to merge

- For our simulation this corresponds to 1.2 seconds for 10Msun and 142 days for 10^8Msun
- The effect is still present in unequal mass binaries, (and BH-NS and NS-NS).

We need full numerical GRMHD simulations

Bonus Track: BBHs Last tango

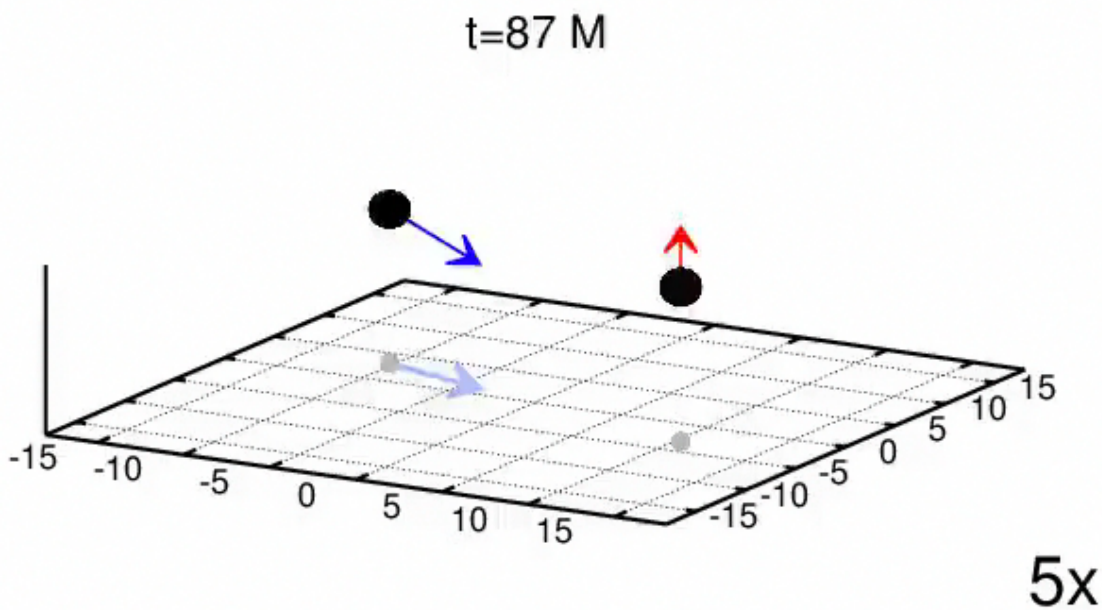

Flip-flops and alignment instability

Flip-Flopping Black Holes: Study of polar oscillations of BH spins

C. O. Lousto and J. Healy, Phys. Rev. Lett. **114**, 141101 (2015), arXiv:1410.3830 [gr-qc].
C. O. Lousto, J. Healy, and H. Nakano, Phys. Rev. **D93**, 044031 (2016), arXiv:1506.04768 [gr-qc].

Up-down spin configurations can be unstable (using low averaged PN)

D. Gerosa, M. Kesden, R. O'Shaughnessy, A. Klein, E. Berti, U. Sperhake, and D. Trifirò, Phys. Rev. Lett. **115**, 141102 (2015), arXiv:1506.09116 [gr-qc].

in between $r_{ud\pm} = (\sqrt{\alpha_2} \pm \sqrt{q\alpha_1})^4 M/(1-q)^2$.

We study the instability here by direct integration of the 3.5PN equations of motion and 2.5PN spins evolutions

C. O. Lousto and J. Healy, Phys. Rev. D **93**, 124074 (2016).

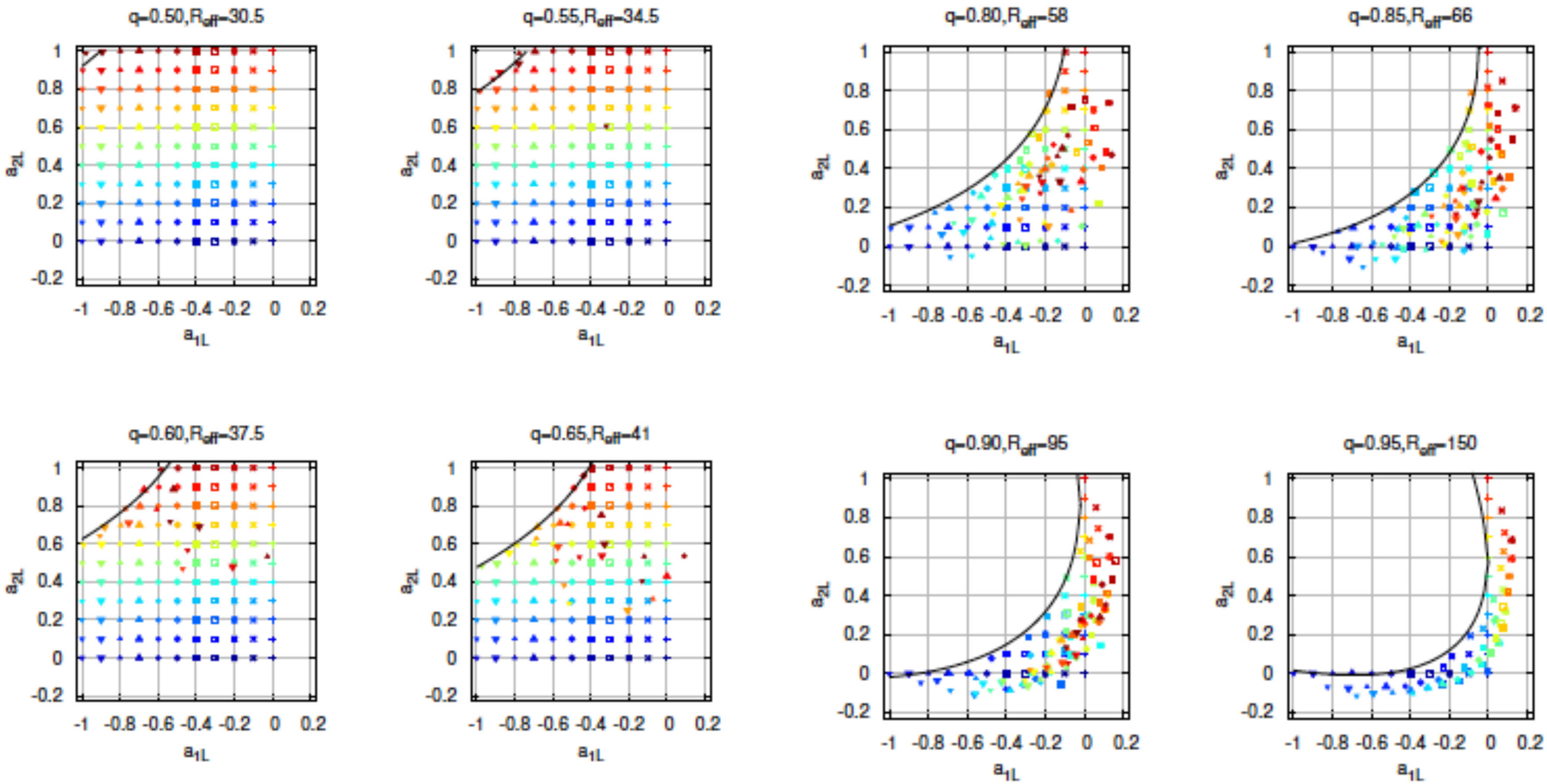

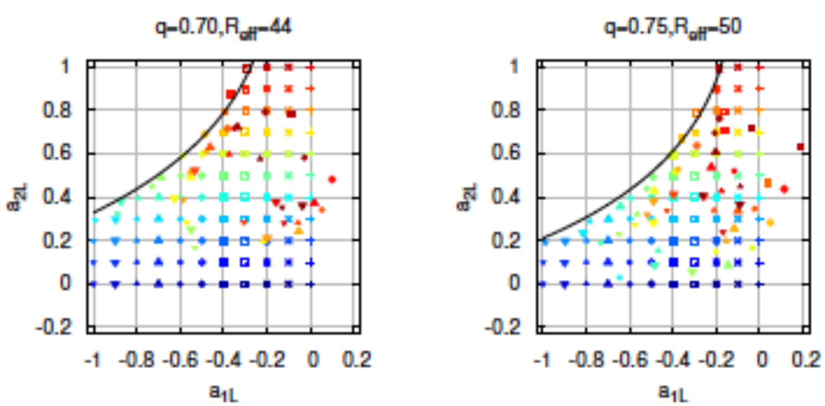

FIG. 1. Snapshots of the spin components along the orbital angular momentum at a binary separation $r/M = 11$. The integration of the PN evolution equations for each binary mass ratio q, started at $r/M > R_c$ with a uniform distribution of spins in the range $0 \leq \alpha_{2L} \leq 1$ for the large BH and $-1 \leq \alpha_{1L} \leq 0$ for the small BH, which was antialigned with the orbital angular momentum by 179-degrees. The color indicates the original value of the spins. The black curve models the depopulation region as given in Eq. (4).

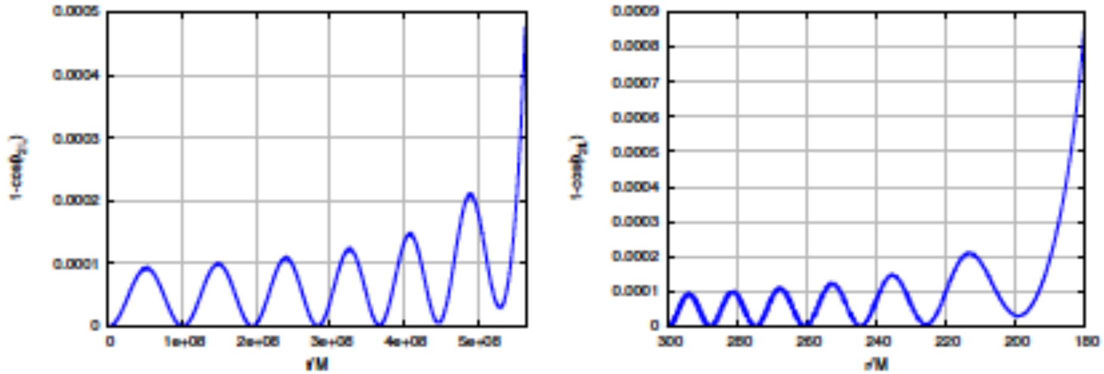

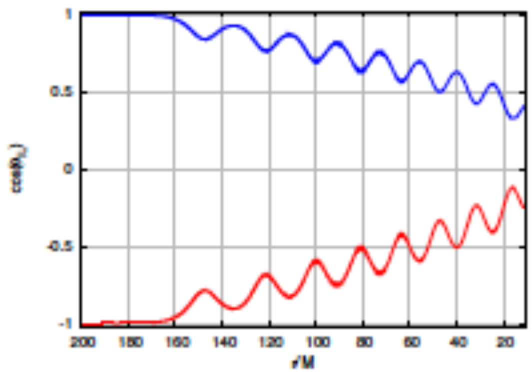

FIG. 2. Evolution of a binary with mass ratio $q = 0.75$, large BH spin $\alpha_{2L} = 1$ initially aligned and small BH spin $\alpha_{1L} = -1$ antialigned with the orbital angular momentum by 179-degrees. The upper panels display the onset of the instability from stable flip-flop oscillations. The middle panels display the development of the instability as the binary separation shrinks. Here $\cos\theta_{iL} = S_{iL}/S_i$ with $i = 1, 2$ for the small, large holes. The lower panels display a polar view of the onset of the misalignment instability.

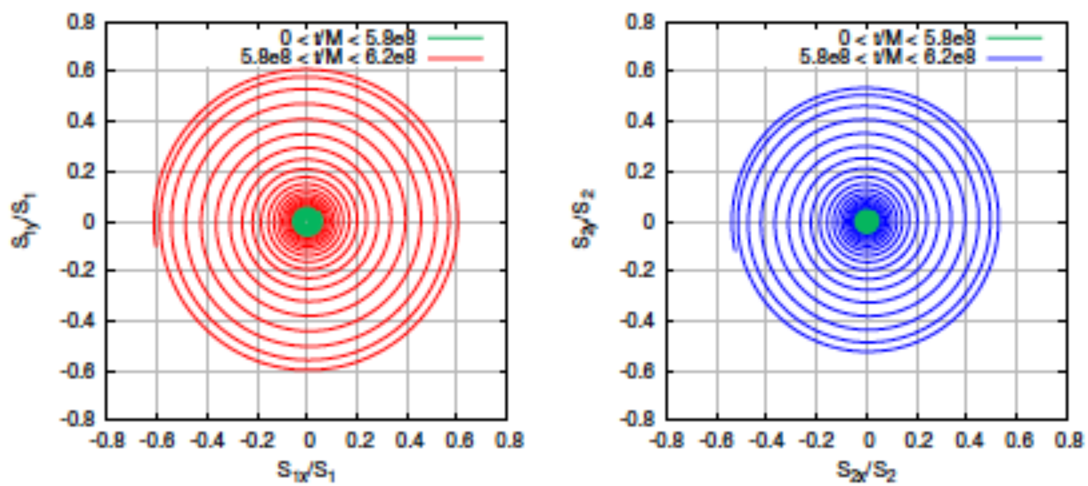

Flip-flop instability

2 PN Analytic study

$$d^2(\vec{S}_i \cdot \hat{L})/dt^2 = -\Omega_{ff}^2\, \vec{S}_i \cdot \hat{L} + \cdots$$

$$\Omega_{ff}^2 = \frac{9}{4}\frac{(1-q)^2 M^3}{(1+q)^2 r^5} + 9\frac{(1-q)(S_{1\hat{L}} - S_{2\hat{L}})M^{3/2}}{(1+q)r^{11/2}} - \frac{9}{4}\frac{(1-q)(3+5q)S_{1\hat{L}}{}^2}{q^2r^6} + \frac{9}{2}\frac{(1-q)^2 S_{1\hat{L}} S_{2\hat{L}}}{qr^6} + \frac{9}{4}\frac{(1-q)(5+3q)S_{2\hat{L}}{}^2}{r^6} + \frac{9}{4}\frac{S_0^2}{r^6} + 9\frac{(1-q)^2 M^4}{(1+q)^2 r^6}, \quad (1)$$

where $\vec{S}_0/M^2 = (1+q)\left[\vec{S}_1/q + \vec{S}_2\right]$.

$$\Omega_{ff}(q, \vec{\alpha}_1, \vec{\alpha}_2, R_c) = 0. \quad (2)$$

The solution of this quadratic equation for antialigned spins leads to two roots $R_c^{\pm}$.

$$R_c^{\pm} = 2M\frac{A \pm 2(\alpha_{2L} - q^2\alpha_{1L})\sqrt{B}}{(1-q^2)^2}, \quad (3)$$

$$A = (1+q^2)(\alpha_{2L}^2 + q^2\alpha_{1L}^2), -2q(1+4q+q^2)\alpha_{1L}\alpha_{2L} - 2(1-q^2)^2$$

$$B = 2(1+q)\left[(1-q)q^2\alpha_{1L}^2 - (1-q)\alpha_{2L}^2 - 2q(1+q)\alpha_{1L}\alpha_{2L} - 2(1-q)^2(1+q)\right].$$

Mass ratio dependence

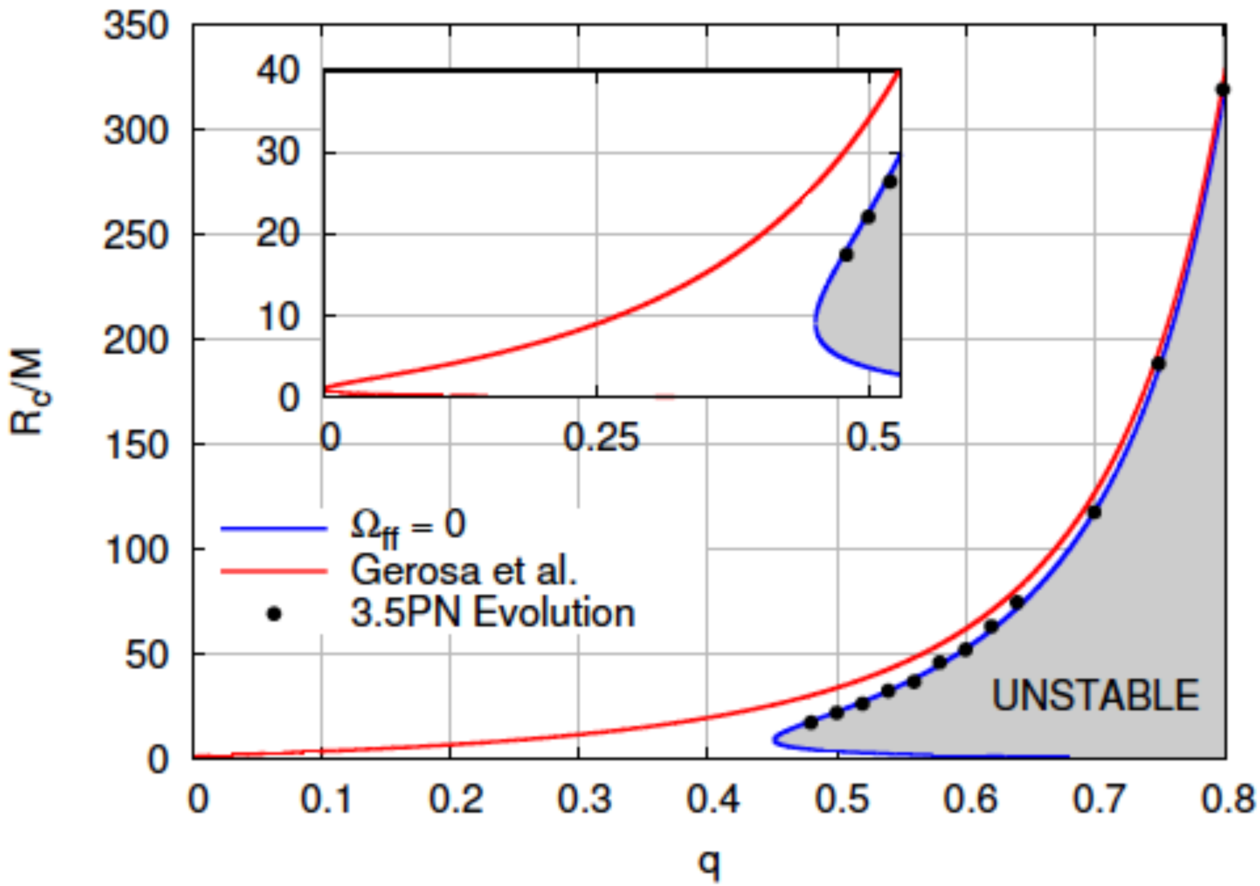

FIG. 3. The instability region, between $R_c^{\pm}$, as a function of the mass ratio, q, as the binary transitions from real to imaginary flip-flop frequencies (blue curve) for maximal spins $\alpha_{1L} = -1$ and $\alpha_{2L} = +1$. For comparison also plotted are $r_{ud\pm}$ from [8] (red curve). The dots correspond to 3.5PN evolutions.

GW150914

In which sense aligned spin templates are representative of more generic systems?

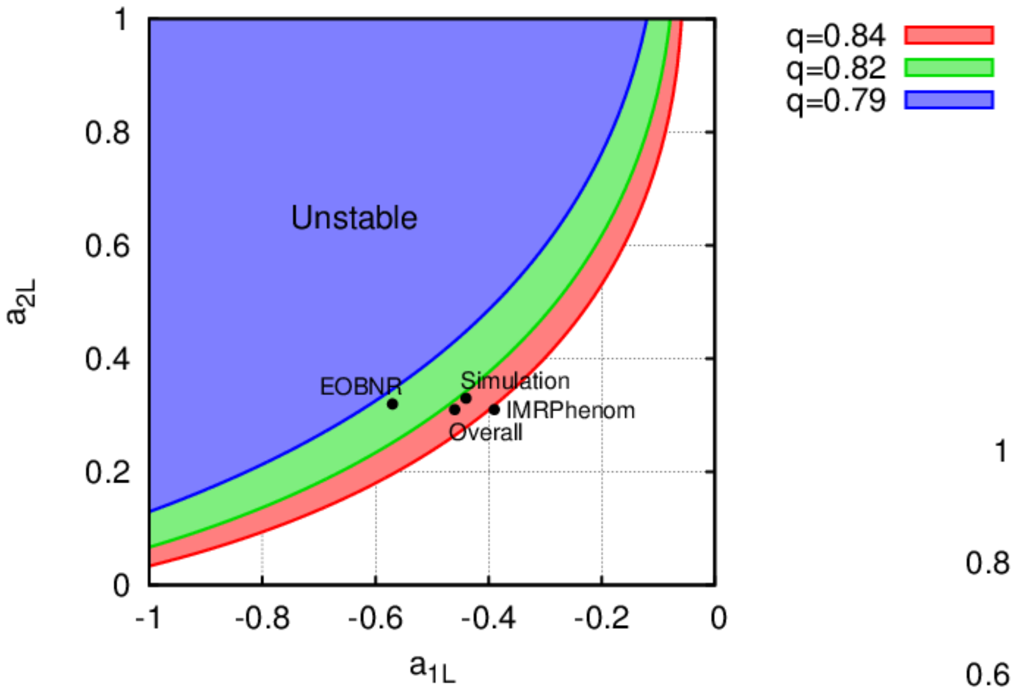

$q = m_1/m_2 = 0.82$
$a_1^L = -0.44$
$a_2^L = +0.33$

Instability map

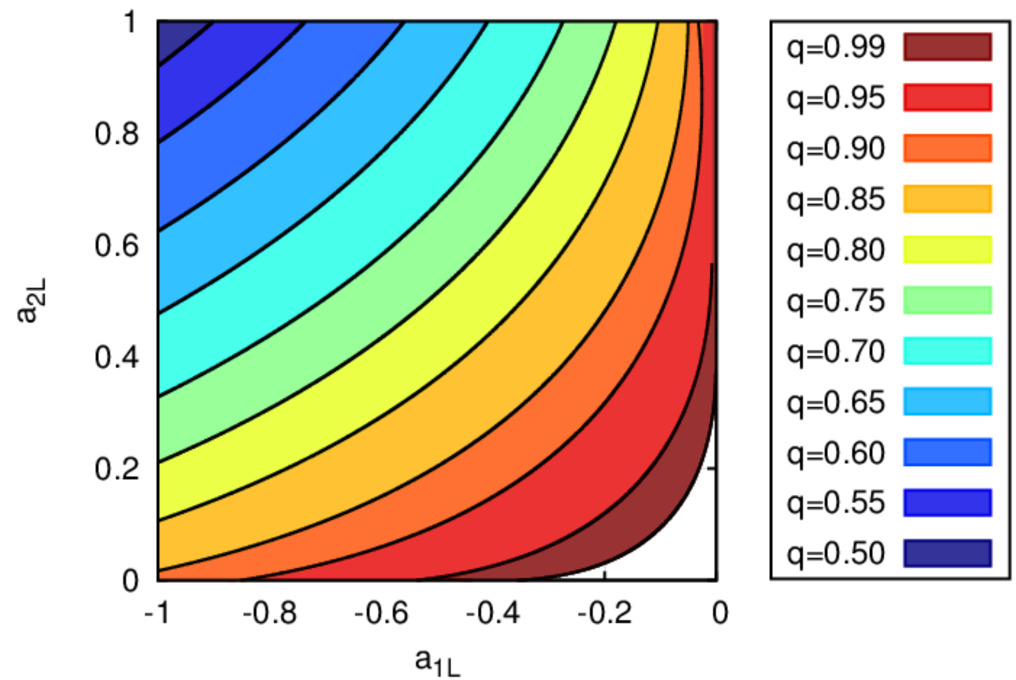

Larger misalignments

Depletion effective for up to 35,45,50 degs. misalig. For q=0.6,0.75,0.90 respectively.

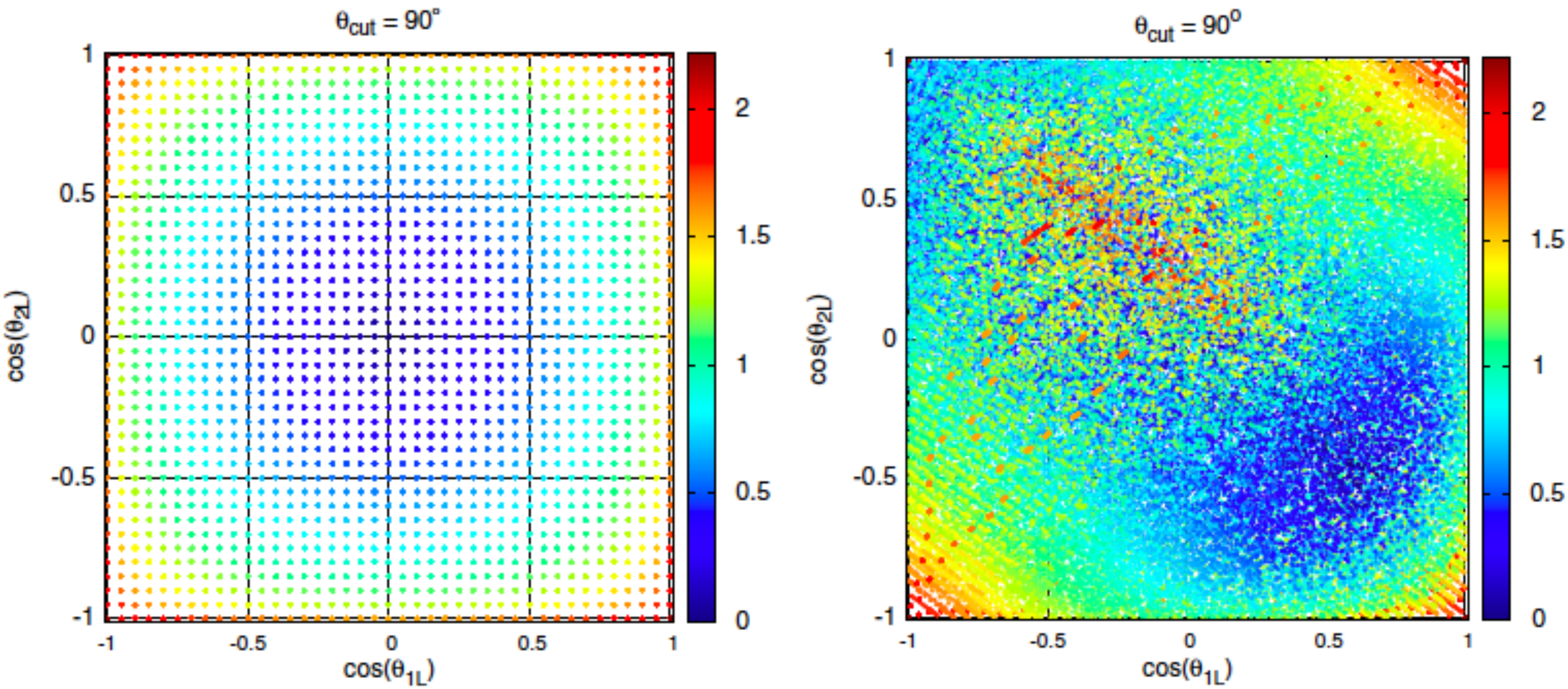

FIG. 4. Upper: Initial configuration of a binary with mass ratio $q = 0.75$ at $r = 500M$ of separation. Color labels angular deviations of the spins from the orbital angular momentum direction $\hat{L}$. Lower: The spin orientations near merger at $r = 11M$ displaying a replenish of the unstable region from the highly misaligned spins.

Discussion

- Flip-flop and instabilities can be seen as a single phenomena of “real” and “imaginary” oscillation frequencies
- Instabilities introduce a notable “dent” into the spins distribution of quasi-aligned binaries
- The instabilities lead to notable changes in the predicted recoil and merger scenario

TABLE I. Initial data parameters and system details for full numerical evolutions. The initial coordinate separation is $D = 11M$ and the intrinsic spins are $\alpha_{1,2}^{x,y,z}$. The eccentricity measured at the end of the inspiral is e_f, and the number of orbits just before merger N. # labels the PN runs that started at binary separation $r = 500M$ with normalized spins (a_1^z, a_2^z).

#	(a_1^z, a_2^z)	q	α_1^x	α_1^y	α_1^z	α_2^x	α_2^y	α_2^z	N	e_f
1	$(-0.8, 0.8)$	0.70	0.7738	0.1876	-0.0775	0.6162	0.4183	0.2921	8.7	0.0037
2	$(-0.4, 0.8)$	0.75	-0.3205	0.2392	0.0070	-0.5926	-0.2040	0.4971	9.6	0.0009
3	$(-0.6, 0.6)$	0.75	0.5467	0.2462	-0.0223	0.4724	0.3311	0.1651	8.4	0.0024
4	$(-0.8, 0.8)$	0.75	0.0559	0.7598	-0.2440	-0.2564	0.6676	0.3585	8.6	0.0052
5	$(-0.8, 0.4)$	0.75	-0.4617	-0.4859	-0.4367	0.0581	-0.3765	0.1220	7.4	0.0040

TABLE II. Remnant properties of the merged black hole. The final mass m_{rem} and spin α_{rem} (normalized to total initial mass) are measured from the horizon, and the recoil velocity (in km/s) is calculated from the gravitational waveforms. Comparison with predicted aligned spins values m_{pre}, $\alpha_{pre}^{x,y,z}$, V_{pre}^{xy}, is based on [13]

#	m_{rem}	m_{pre}	α_{rem}^x	α_{rem}^y	α_{rem}^z	α_{pre}^z	V_{rem}^x	V_{rem}^y	V_{rem}^z	V_{pre}^{xy}
1	0.9445	0.9456	0.2712	0.1445	0.7464	0.7742	-3.9	28.7	-133.7	260.7
2	0.9408	0.9409	-0.1920	-0.0451	0.7909	0.7994	273.5	-24.9	-775.8	187.7
3	0.9485	0.9486	0.1994	0.1155	0.7216	0.7388	138.1	-11.2	557.8	200.4
4	0.9468	0.9462	-0.0685	0.2650	0.7591	0.7601	5.9	117.0	241.7	282.9
5	0.9534	0.9546	-0.0610	-0.1458	0.6683	0.6752	47.6	-11.1	386.4	201.7